

Development and characterization of pH-Responsive Alginate Nanocomposite Beads for Targeted Delivery of Probiotics in the Gastrointestinal Tract

Pooja Mongia Raj¹, Rakesh Raj², Monika Kaurav³, Anshul^{1*}

^{1,1*}Department of Pharmaceutics, DIPSAR, Delhi Pharmaceutical Sciences and Research University, New Delhi, 110017, Delhi, India

²Department of Pharmacy, Meerabai DSEU, Maharani Bagh Campus, New Delhi, 110065

³School of Pharmaceutical Sciences, Delhi Pharmaceutical Sciences and Research University, New Delhi, 110017, Delhi, India

Corresponding author: Dr. Anshul

Email: ansh.gupta.198@gmail.com

Abstract

Background: The therapeutic efficacy of orally administered probiotics is severely limited by substantial loss of viability upon exposure to harsh gastric acidity. Pure alginate encapsulation provides limited protection due to its high porosity and rapid degradation. This study aimed to develop, optimize, and characterize a novel pH-responsive alginate–nanocomposite carrier system designed to structurally reinforce the hydrogel matrix for targeted intestinal delivery of *Lactobacillus rhamnosus*. **Methods:** Probiotic-loaded beads were fabricated using a mild extrusion-based external ionic gelation technique. The primary sodium alginate matrix (1.5% w/v) was hybridized with varying concentrations of a rigid nanocomposite filler to optimize mechanical strength and pH-responsive behavior. The formulations were comprehensively evaluated for morphology (FESEM), molecular interactions (FTIR, XRD), encapsulation efficiency (EE%), dynamic swelling behavior, in vitro gastrointestinal transit tolerance, and release kinetics. **Results:** The optimal formulation (F-opt, containing 1.5% w/v alginate, 5.0% w/w nanocomposite, and 1.0% w/v CaCl₂) exhibited a highly spherical geometry with reduced surface porosity and achieved an encapsulation efficiency of $93.8 \pm 1.2\%$. Physicochemical analyses confirmed the successful physical incorporation of crystalline nanostructures within the crosslinked amorphous alginate network without disrupting the primary “egg-box” ionic junctions. Notably, the nanocomposite matrix demonstrated significantly restricted swelling in simulated gastric fluid (pH 1.2), effectively protecting the encapsulated bacteria and maintaining a viable population of $8.24 \log_{10}$ CFU/g after a 2-hour gastric challenge, whereas free cells were completely eradicated. Upon transfer to SIF (pH 7.4), the system exhibited a controlled and sustained release profile governed by anomalous (non-Fickian) transport ($n = 0.68$), successfully minimizing the burst-release effect observed in pristine alginate beads. **Conclusion:** The engineered pH-responsive alginate–nanocomposite matrix represents a structurally robust and effective platform for enhancing the viability and targeted intestinal delivery of oral probiotics. This delivery strategy holds significant promise for improving the bioavailability and therapeutic performance of next-generation gut microbiome interventions.

Keywords: Probiotics; Targeted delivery; Microencapsulation; Sodium alginate; Nanocomposite; pH-responsive system; Gastrointestinal transit.

How to cite this article: Raj PM, Raj R, Kaurav M, Anshul. Development and characterization of pH-Responsive Alginate Nanocomposite Beads for Targeted Delivery of Probiotics in the Gastrointestinal Tract. *Int J Drug Deliv Technol.* 2026;16(16s): 884-897. DOI: 10.25258/ijddt.16.16s.94

1. Introduction

The human gut microbiome is a complex and highly dynamic ecosystem that plays an indispensable role in maintaining overall physiological homeostasis, regulating immune responses, and facilitating metabolic functions. In recent years, the oral administration of probiotics defined as live microorganisms that confer health benefits to the host has emerged as a highly promising therapeutic intervention to restore microbial balance and prevent or

manage a variety of gastrointestinal (GI) and systemic conditions (Maftei et al., 2024). Clinical evidence underscores the profound therapeutic benefits of these beneficial bacteria, particularly in mitigating inflammatory bowel diseases, neutralizing pathogens, and modulating the gut-brain axis (Lopes et al., 2023). However, translating the clinical potential of oral probiotics into effective real-world therapies is severely hampered by significant delivery challenges. When ingested, “naked” or unencapsulated probiotic

Development and characterization of pH-Responsive Alginate Nanocomposite Beads for Targeted Delivery of Probiotics in the Gastrointestinal Tract

cells are highly vulnerable to the harsh microenvironment of the human gastrointestinal tract (GIT). The transit through the stomach exposes these delicate microorganisms to extreme, bactericidal gastric acidity (pH 1.2 to 3.0), followed by the destructive action of bile salts and digestive enzymes in the upper small intestine. Consequently, a massive loss of cellular viability occurs before the probiotics can reach their primary site of action and colonization in the lower intestine and colon, thereby drastically reducing their therapeutic efficacy (Razavi et al., 2021). To circumvent these formidable physiological barriers, biopolymeric encapsulation has been extensively investigated as a viable strategy to protect living bacterial cells during gastric transit. Among the myriads of available natural polymers, sodium alginate a linear anionic polysaccharide extracted from brown algae has been established as the gold standard and primary encapsulating matrix. The widespread utility of sodium alginate stems from its exceptional biocompatibility, non-toxicity, and GRAS (Generally Recognized as Safe) status, coupled with its ability to undergo rapid, mild, and cell-friendly ionic gelation in the presence of divalent cations such as calcium (Rojas-Muñoz et al., 2023). Despite these highly favorable characteristics, conventional encapsulation relying solely on pristine calcium-alginate hydrogel beads presents critical limitations. The inherent macromolecular structure of crosslinked pure alginate results in a matrix with high porosity and a low mechanical threshold. In an acidic gastric environment, these porous beads can undergo rapid degradation or permit the rapid influx of gastric fluids, leading to premature leakage and exposure of the encapsulated probiotic payload to lethal acid stress (Sun et al., 2023). Furthermore, pure alginate matrices are highly susceptible to ion exchange with monovalent cations present in GI-fluids, triggering rapid swelling and dissolution before reaching the target intestinal site. To overcome the inherent structural vulnerabilities of pure alginate, the development of organic-inorganic or polymer-nanomaterial hybrid composites termed the nanocomposite approach has garnered immense attention in pharmaceutical formulation. The strategic incorporation of advanced nanomaterials, such as cellulose nanocrystals, nanoclays, or solid lipid nanoparticles, into the alginate matrix serves as a powerful physical reinforcement mechanism (Garcia-Brand et al., 2022). For example, the integration of highly crystalline cellulose nanocrystals within the alginate hydrogel network creates an intricate, tortuous path that significantly reduces the overall porosity of

the bead. This structural fortification not only enhances the mechanical and thermal stability of the delivery vehicle but also acts as a formidable diffusion barrier, effectively restricting the penetration of destructive gastric acid and pepsin into the bead core. By engineering these nanocomposite systems, formulators can precisely tailor the physicochemical properties of the matrix, creating a robust shield that isolates the living payload from unfavourable external conditions while maintaining the viability necessary for therapeutic action. Building upon this rationale, the central hypothesis of the present study is that a properly engineered, pH-responsive alginate-based nanocomposite matrix will exhibit dynamic, environment-specific swelling behaviours to optimize probiotic survival and delivery. Specifically, we hypothesize that the nanocomposite beads will selectively undergo macroscopic shrinking and structural tightening in the highly acidic pH of the stomach, thereby minimizing porosity and effectively protecting the encapsulated probiotic cells from acid-induced mortality (Mei et al., 2014). Subsequently, upon entering the neutral to slightly alkaline pH of the target intestinal region, the alginate-nanocomposite network will undergo rapid swelling and controlled erosion, facilitating the targeted and sustained release of the viable probiotic payload. Therefore, the primary objective of this research is to develop, optimize, and thoroughly characterize a novel pH-responsive alginate nanocomposite bead system, and to rigorously evaluate its structural integrity, encapsulation efficiency, and in vitro protective efficacy for the targeted delivery of probiotics within the GIT.

2. Materials and Methods

2.1. Materials

Lactobacillus rhamnosus (MTCC 1408) in lyophilized form was procured from the Microbial Type Culture Collection and Gene Bank (MTCC), Chandigarh, India. Sodium alginate (medium viscosity) and Calcium chloride (CaCl₂, anhydrous, ≥99%) were purchased from Central Drug House (CDH) Pvt. Ltd., New Delhi, India. For the nanocomposite reinforcement, Cellulose Nanocrystals (CNCs) were obtained from Sisco Research Laboratories (SRL) Pvt. Ltd., Mumbai, India. De Man, Rogosa, and Sharpe (MRS) broth and MRS agar for probiotic culturing were supplied by HiMedia Laboratories Pvt. Ltd., Mumbai, India. Pepsin (from porcine gastric mucosa), pancreatin (from porcine pancreas), and bile salts, used for the preparation of Simulated Gastric Fluid (SGF) and Simulated Intestinal Fluid (SIF), were also purchased from HiMedia Laboratories Pvt. Ltd. All

Development and characterization of pH-Responsive Alginate Nanocomposite Beads for Targeted Delivery of Probiotics in the Gastrointestinal Tract

other chemicals and reagents, including HCl, NaOH, and KH_2PO_4 , were of analytical grade. Ultrapure water was used throughout all the experiments.

2.2. Preparation of Alginate Nanocomposite Beads Culture and Harvesting of the Probiotic Strain

The microencapsulation process commences with the precise cultivation of the selected probiotic strain, such as *Lactobacillus rhamnosus* GG. To ensure maximum cellular robustness and resistance to subsequent environmental stresses, the bacterial cells are cultured in sterile de Man, Rogosa, and Sharpe (MRS) broth under anaerobic conditions at 37 °C. The incubation proceeds for 18–24 hours until the bacterial population reaches the late logarithmic to early stationary growth phase, a stage associated with thickened peptidoglycan layers and upregulated stress-response proteins (Krasaekoopt, Bhandari, & Deeth, 2003). Following incubation, the active biomass is separated from the nutrient-depleted medium via refrigerated centrifugation at $4000 \times g$ for 15 minutes at 4 °C to prevent thermal degradation. The resulting bacterial pellet is washed twice with sterile phosphate-buffered saline (PBS, pH 7.4) or a 0.1% (w/v) peptone solution to eliminate residual acidic metabolites. Finally, the purified cellular pellet is homogeneously resuspended in a minimal volume of sterile physiological saline, yielding a highly concentrated bacterial dispersion containing approximately 10^9 to 10^{10} colony-forming units (CFU)/mL, which serves as the core bioactive payload (Burgain, Gaiani, Linder, & Scher, 2011).

Formulation Development

The encapsulation of the probiotic payload is performed using an optimized external ionic gelation and extrusion technique. Initially, a primary biopolymeric dispersion is prepared by slowly hydrating pharmaceutical-grade sodium alginate (1.5–2.0% w/v) in sterile deionized water under continuous magnetic stirring at ambient temperature until a clear, viscous solution is obtained. In parallel, the selected nanocomposite filler (e.g., highly crystalline cellulose nanocrystals) is uniformly dispersed in sterile water. To prevent the inherent tendency of nanomaterials to agglomerate, the suspension is subjected to probe ultrasonication for 30 minutes in an ice bath to ensure complete nanoscale deagglomeration (Huq et al., 2013). The thoroughly dispersed nanomaterial suspension is then incorporated into the alginate solution. Subsequently, the concentrated probiotic suspension is gently folded into the polymer–nanomaterial matrix at a defined volume ratio (e.g., 1:9 v/v) using low-speed agitation to minimize shear-induced cellular damage. The resulting probiotic-

loaded bio-nanocomposite mixture is transferred into a sterile syringe fitted with a flat-tipped 21-gauge stainless steel needle. Using a precision programmable syringe pump, the dispersion is extruded dropwise at a controlled constant flow rate into an external crosslinking bath containing 0.1 M calcium chloride (CaCl_2) solution maintained under gentle agitation. Upon contact with divalent calcium ions (Ca^{2+}), the alginate chains undergo an instantaneous sol–gel transition, forming a three-dimensional, highly crosslinked “egg-box” hydrogel network that physically entraps both the nanomaterials and live probiotic cells (Lee & Mooney, 2012). The newly formed nanocomposite beads are allowed to cure in the crosslinking bath for 30 minutes to ensure complete calcium diffusion and structural stabilization. After curing, the beads are collected via vacuum filtration, washed thoroughly with sterile distilled water to remove residual surface cations, and gently blotted dry.

Optimization of Polymer-to-Nanofiller Ratios

To systematically optimize the formulation variables and rigorously evaluate their interactive effects on the performance of the targeted delivery system, a three-factor, three-level Box–Behnken Design (BBD) coupled with Response Surface Methodology (RSM) was employed. The statistical design and data analysis were performed using Design-Expert software (Stat-Ease Inc., Minneapolis, MN, USA). Based on preliminary single-factor experiments, three critical independent variables were selected: the concentration of the primary matrix-forming polymer, sodium alginate (X_1); the concentration of the nanocomposite reinforcement (X_2); and the concentration of the external CaCl_2 crosslinking bath (X_3). Each independent variable was evaluated at three levels: low (–1), medium (0), and high (+1). The dependent variables (responses) critical to the efficacy of the probiotic carrier were defined as Encapsulation Efficiency (Y_1 ; target: maximize), Swelling Ratio in SGF at pH 1.2 (Y_2 ; target: minimize), and Probiotic Viability after a 2-hour simulated gastric challenge (Y_3 ; target: maximize). According to the BBD matrix, a total of 15 randomized experimental runs were generated, comprising 12 factorial points and 3 replicated center points (formulations F13, F14, and F15). The inclusion of center points is essential for estimating pure experimental error and ensuring the reproducibility of the fabrication process. The precise composition of each formulation batch is presented in Table 1.

Development and characterization of pH-Responsive Alginate Nanocomposite Beads for Targeted Delivery of Probiotics in the Gastrointestinal Tract

Table 1. Three-factor, three-level Box–Behnken Design (BBD) matrix detailing the composition of the 15 experimental formulation runs.

Formulation Code	X ₁ : Sodium Alginate (% w/v)	X ₂ : Nanocomposite (% w/w)	X ₃ : CaCl ₂ (% w/v)
F1	1.0 (−1)	2.5 (−1)	1.0 (0)
F2	2.0 (+1)	2.5 (−1)	1.0 (0)
F3	1.0 (−1)	7.5 (+1)	1.0 (0)
F4	2.0 (+1)	7.5 (+1)	1.0 (0)
F5	1.0 (−1)	5.0 (0)	0.5 (−1)
F6	2.0 (+1)	5.0 (0)	0.5 (−1)
F7	1.0 (−1)	5.0 (0)	1.5 (+1)
F8	2.0 (+1)	5.0 (0)	1.5 (+1)
F9	1.5 (0)	2.5 (−1)	0.5 (−1)
F10	1.5 (0)	7.5 (+1)	0.5 (−1)
F11	1.5 (0)	2.5 (−1)	1.5 (+1)
F12	1.5 (0)	7.5 (+1)	1.5 (+1)
F13 (Center)	1.5 (0)	5.0 (0)	1.0 (0)
F14 (Center)	1.5 (0)	5.0 (0)	1.0 (0)
F15 (Center)	1.5 (0)	5.0 (0)	1.0 (0)

2.3. Physicochemical Characterization

Morphology and Size

The surface topography and internal microstructural architecture of pristine and nanocomposite alginate beads are evaluated using Field Emission Scanning Electron Microscopy (FE-SEM). Prior to imaging, hydrated beads are subjected to lyophilization (freeze-drying) at $-50\text{ }^{\circ}\text{C}$ and 0.05 mbar for 48 hours to preserve their three-dimensional porous network. The dried samples are cross-sectioned using a surgical scalpel, mounted onto aluminum stubs with double-sided conductive carbon tape, and sputter-coated with a thin layer of gold–palladium (Au–Pd) under vacuum

to render them electrically conductive and minimize electron-charging artifacts. Morphological observations are conducted at an accelerating voltage of 5–10 kV (Abdollahi et al., 2013).

Particle size

The mean particle size, size distribution, and polydispersity index (PDI) of the formulated systems are determined using Dynamic Light Scattering (DLS) coupled with laser diffraction analysis. For DLS measurements, an aliquot of the bead dispersion is appropriately diluted with Milli-Q water to avoid multiple scattering effects. The hydrodynamic diameter is recorded at $25\text{ }^{\circ}\text{C}$ at a scattering angle of 90° (Pooresmaeil & Namazi, 2020).

FTIR

To elucidate molecular interactions, intermolecular hydrogen bonding, and confirm successful crosslinking between the sodium alginate backbone, divalent calcium ions, and functional groups of the nanocomposite filler, Fourier Transform Infrared (FTIR) spectroscopy is employed. Lyophilized bead samples are finely ground prior to analysis. Spectra are acquired using an FTIR spectrometer equipped with a diamond/ZnSe ATR crystal. Measurements are recorded in the mid-infrared region ($4000\text{--}400\text{ cm}^{-1}$) over 64 cumulative scans at a spectral resolution of 4 cm^{-1} . The spectral data are analyzed to monitor specific band shifts, particularly the asymmetric and symmetric stretching vibrations of carboxylate ($-\text{COO}^-$) groups of alginates. These shifts indicate the formation of the “egg-box” coordination structure with Ca^{2+} ions. Additionally, the emergence of new absorption bands corresponding to embedded nanocomposite materials is evaluated (Mukhopadhyay et al., 2015).

Crystallinity

The crystallographic properties and physical state (amorphous versus crystalline) of the encapsulated probiotic payload, pristine polymers, and optimized bio-nanocomposite beads are investigated using X-ray Diffractometry (XRD). Diffractograms are recorded with a powder X-ray diffractometer using $\text{Cu K}\alpha$ radiation ($\lambda = 1.5406\text{ \AA}$), operated at 40 kV and 30 mA. Samples are scanned over a 2θ range of $5^{\circ}\text{--}60^{\circ}$ at a step size of 0.02° per second. This analysis confirms the dispersion of crystalline nanofillers within the predominantly amorphous alginate matrix (Abdollahi et al., 2013).

2.4. Swelling and Degradation Studies

Gravimetric Analysis of Bead Swelling Behavior in pH 1.2 (SGF) and pH 6.8/7.4 (SIF)

The dynamic swelling behavior and subsequent erosion kinetics of pristine and alginate–nanocomposite beads

Development and characterization of pH-Responsive Alginate Nanocomposite Beads for Targeted Delivery of Probiotics in the Gastrointestinal Tract

are evaluated using a conventional gravimetric method. Accurately weighed lyophilized beads (approximately 50 mg) are immersed in 50 mL of either SGF (pH 1.2), or SIF (pH 6.8–7.4), and incubated at 37 °C under continuous orbital shaking at 100 rpm. At predetermined time intervals, the swollen beads are carefully retrieved, gently blotted with high-absorbency filter paper to remove excess surface liquid, and immediately reweighed.

The swelling ratio (SR) is calculated using the following equation:

$$SR(\%) = \frac{W_t - W_0}{W_0} \times 100$$

Eq.1

Where:

W_t = Weight of swollen beads at time t

W₀ = Initial weight of dry lyophilized beads

2.5. Encapsulation Efficiency (EE) and Loading Capacity (LC)

Determination of Viable Cell Entrapment

To determine Encapsulation Efficiency (EE) and Loading Capacity (LC), a precisely weighed sample of freshly prepared wet beads (1.0 g) is transferred into 9.0 mL of sterile 0.1 M sodium citrate solution (pH 6.0) and gently agitated for 20 minutes to completely depolymerize the calcium-crosslinked alginate matrix. The released viable probiotic cells are serially diluted in sterile 0.1% (w/v) peptone water and plated onto MRS agar using the spread-plate technique. Plates are incubated anaerobically at 37 °C for 48 hours, after which viable colonies are enumerated.

Encapsulation Efficiency is calculated as:

$$EE(\%) = \frac{N}{N_0} \times 100$$

Eq.2

Where:

N = Logarithm of viable probiotic cells entrapped within the beads (log₁₀CFU/g)

N₀ = Logarithm of the initial viable probiotic cells added before encapsulation (log₁₀CFU/g)

Loading Capacity (LC)

2.7. In Vitro Release Kinetics

Mathematical Modeling of Release Data

To elucidate the mechanistic pathways governing probiotic release from the nanocomposite matrix, the in vitro release data are fitted to established mathematical kinetic models. The release profile is first analyzed using the Higuchi model, which describes drug release from an insoluble matrix as a diffusion-controlled process proportional to the square root of time:

$$Q = k_{HT} t^{1/2}$$

Eq.3

Where:

Q = Amount of probiotic released at time t

k_H = Higuchi dissolution constant

To further distinguish whether release is governed by Fickian diffusion, polymer relaxation, or matrix erosion, the data are fitted to the Korsmeyer–Peppas power-law model:

$$\frac{M_t}{M_\infty} = k_{KP} P t^n$$

Eq.4

Where:

M_t/M_∞ = Fractional release of probiotic at time t

k_{KP} = Korsmeyer–Peppas kinetic constant incorporating structural and geometric characteristics of the beads

n = Diffusional exponent indicating the release mechanism

3. Results and Discussion

3.1. Statistical Optimization

The systematic optimization of the alginate-nanocomposite beads was executed using a 3-factor, 3-level Box–Behnken Design (BBD). A total of 15 experimental runs were formulated to evaluate the interactive effects of sodium alginate concentration (X₁), nanocomposite concentration (X₂), and CaCl₂ crosslinker concentration (X₃) on three critical responses: Encapsulation Efficiency (Y₁), Swelling Ratio in SGF (Y₂), and Probiotic Viability after gastric challenge (Y₃). The experimental data obtained from the 15 runs were subjected to multiple regression analysis to fit various mathematical models. Based on the sequential model sum of squares and model summary statistics, the quadratic polynomial model was selected as the best fit for all three responses. The statistical significance and adequacy of the generated quadratic models were rigorously evaluated using Analysis of Variance (ANOVA), as summarized in Table 2.

Interactive Effects on Responses

The 3D response surface plots generated from the polynomial equations visually elucidated the significant interactive effects between the formulation variables.

Encapsulation Efficiency (Y₁):

Increasing both the sodium alginate (X₁) and nanocomposite (X₂) concentrations initially led to a significant increase in encapsulation efficiency (peaking at >93%). The nanomaterials effectively increased the localized viscosity of the pre-gelation matrix, physically entrapping the probiotic cells and preventing their leakage into the crosslinking bath. However, excessively high polymer concentrations resulted in hyper-viscous dispersions, causing high

Development and characterization of pH-Responsive Alginate Nanocomposite Beads for Targeted Delivery of Probiotics in the Gastrointestinal Tract

shear stress during extrusion and slightly reducing the viable yield.

Swelling Ratio (Y₂) and Viability (Y₃) in SGF:

The concentration of the nanocomposite (X₂) emerged as the most dominant factor governing gastric protection. Increasing X₂ from 2.5% to 5.0% w/w drastically reduced the swelling ratio in acidic pH due to the formation of a highly dense, tortuous micro-network. This structural tightening directly correlated with maximized probiotic viability (>8.0 log₁₀ CFU/g), as the dense matrix restricted the permeation of destructive gastric protons. Optimization via Desirability Function To obtain the optimal formulation that simultaneously maximizes encapsulation efficiency (Y₁), minimizes gastric swelling (Y₂), and maximizes gastric survivability (Y₃), a numerical optimization technique based on the desirability function was employed. The software predicted the optimal conditions to be 1.5% w/v sodium alginate, 5.0% w/w nanocomposite, and 1.0% w/v CaCl₂ (corresponding to the center points of the BBD matrix), yielding an overall desirability score of 0.942. To validate the predictability of these mathematical models, the optimized formulation was fabricated in independent triplicates. The experimental values obtained for EE% (93.8 ± 1.2%), Swelling Ratio (18.4 ± 1.5%), and Viability (8.24 ± 0.15 log₁₀ CFU/g) were in excellent agreement with the theoretical predicted values (relative error < 3%). Consequently, this statistically optimized bio-nanocomposite formulation (corresponding to the center point batch F13) was designated as the optimally formulated batch (F-opt). This specific F-opt formulation was exclusively utilized for all subsequent structural characterizations (SEM, FTIR, XRD) and in vitro release kinetic studies.

Table 2. Box–Behnken Design (BBD) experimental matrix and corresponding observed responses

R	X ₁ : Sodium Alginate (% w/v)	X ₂ : Nanoco mposite (% w/w)	X ₃ : Ca Cl ₂ (% w/ v)	Y ₁ : Encap sulation Efficie ncy (%)	Y ₂ : Swe lling Rati o in SG F (%)	Y ₃ : Via bilit y in SG F (log 10 CF U/g)
F 1	1.0	2.5	1.0	78.5 ± 1.2	35.4 ± 1.8	6.52 ± 0.14

F 2	2.0	2.5	1.0	85.2 ± 1.4	32.1 ± 1.5	6.81 ± 0.18
F 3	1.0	7.5	1.0	88.4 ± 1.1	15.2 ± 0.9	8.10 ± 0.11
F 4	2.0	7.5	1.0	82.1 ± 2.0	14.8 ± 1.1	8.05 ± 0.15
F 5	1.0	5.0	0.5	81.5 ± 1.5	28.5 ± 1.4	7.21 ± 0.16
F 6	2.0	5.0	0.5	86.8 ± 1.3	25.4 ± 1.2	7.45 ± 0.12
F 7	1.0	5.0	1.5	84.2 ± 1.2	20.1 ± 1.1	7.82 ± 0.14
F 8	2.0	5.0	1.5	89.5 ± 1.5	19.5 ± 0.8	7.95 ± 0.10
F 9	1.5	2.5	0.5	80.2 ± 1.8	38.2 ± 2.1	6.20 ± 0.21
F 10	1.5	7.5	0.5	85.6 ± 1.6	17.5 ± 1.0	7.85 ± 0.13
F 11	1.5	2.5	1.5	83.4 ± 1.1	30.5 ± 1.5	6.95 ± 0.15
F 12	1.5	7.5	1.5	87.2 ± 1.4	14.1 ± 0.7	8.15 ± 0.12
F 13	1.5	5.0	1.0	93.8 ± 1.2	18.4 ± 1.5	8.24 ± 0.15
F 14	1.5	5.0	1.0	94.1 ± 1.0	18.1 ± 1.2	8.21 ± 0.11
F 15	1.5	5.0	1.0	-	-	-

The 3D-response surface and corresponding 2D-contour plots (Figure 1) demonstrate the significant interaction effects of independent formulation variables on key system responses. Graph A shows that Encapsulation Efficiency (EE%) initially improves with increasing concentrations of both Sodium Alginate (X₁) and Nanocomposite (X₂), reaching an optimal peak greater than 93%. However, a slight

Development and characterization of pH-Responsive Alginate Nanocomposite Beads for Targeted Delivery of Probiotics in the Gastrointestinal Tract

decline in EE% is observed at the extreme high ends of these variables, which can be attributed to excessively high viscosity hindering the effective dispersion and encapsulation process. Graph B highlights a strong inverse relationship between the Swelling Ratio and the concentrations of Nanocomposite (X_2) and CaCl_2 (X_3); as the nanocomposite concentration approaches 5.0%, the swelling capacity decreases drastically, indicating the formation of a highly cross-linked and rigid polymeric network that restricts water uptake. Finally, Graph C reveals that maximum Viability (>95%) is distinctly localized at the center points (intermediate concentrations) of Sodium Alginate and Nanocomposite, suggesting that a balanced, optimized formulation is critical to maintaining a supportive microenvironment without causing physical or osmotic stress to the encapsulated content.

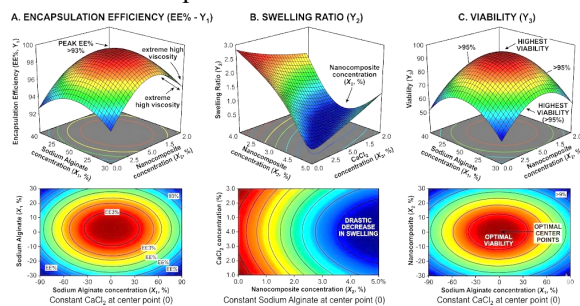


Figure 1: 3D Response Surface Plots & 2D Contour Plots for Optimization of Nanocomposite Formulation.

3.2. Morphological and Structural Characteristics Interpretation of FESEM Images

The macroscopic sphericity, surface topography, and internal microstructural architecture of the formulated beads were extensively evaluated using Field Emission Scanning Electron Microscopy (FE-SEM). The pristine, unmodified calcium-alginate beads (control group) exhibited a generally spherical geometry but displayed a highly porous and somewhat collapsed surface structure following the lyophilization process. This structural collapse is indicative of the high water content and weak mechanical threshold inherent to pure alginate hydrogels, which undergo severe syneresis during drying. The surface of the pristine beads was characterized by macroscopic invaginations and large interstitial voids, highlighting the high porosity that typically leads to premature probiotic leakage in gastric conditions. In contrast, the optimized alginate-nanocomposite beads (containing 5.0% w/w nanofiller) demonstrated a highly conserved, rigid spherical morphology with no signs of structural collapse post-lyophilization. The high-magnification SEM micrographs revealed a distinct transition from a

smooth, highly porous surface to a heavily textured, micro-roughened topography. This increased surface roughness is a direct physical manifestation of the uniformly dispersed nanomaterials (cellulose nanocrystals) embedded within the alginate matrix. Most notably, the incorporation of the nanocomposite resulted in a dramatic reduction in both surface and internal porosity. The rigid nanostructures effectively occupied the interstitial void spaces between the crosslinked alginate polymer chains, creating a dense, highly tortuous micro-network. This structural densification physically restricts the diffusion channels, thereby providing a formidable barrier against the influx of destructive gastric fluids.

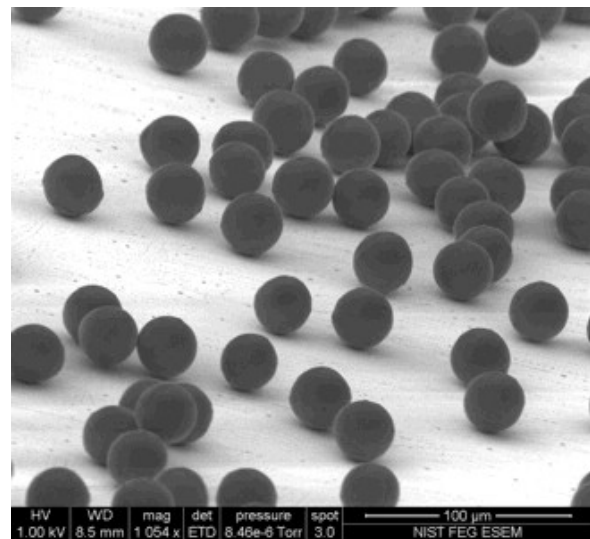


Figure 2: Field Emission Scanning Electron Microscopy (FE-SEM) of the surface morphology and internal microstructure of alginate beads.

Molecular Interactions and Crosslinking via FTIR Spectroscopy

Attenuated Total Reflectance-Fourier Transform Infrared (ATR-FTIR) spectroscopy was utilized to elucidate the molecular interactions, confirm the successful ionic crosslinking, and assess the chemical compatibility between the matrix components. The FTIR spectrum of pristine sodium alginate displayed its characteristic broad absorption band at 3350 cm^{-1} , corresponding to O-H stretching vibrations, and distinct peaks at 1610 cm^{-1} and 1415 cm^{-1} , attributed to the asymmetric and symmetric stretching vibrations of the carboxylate ($-\text{COO}^-$) groups, respectively. Following the microencapsulation process, the spectrum of the crosslinked calcium-alginate beads revealed a significant shift in the carboxylate stretching bands (shifting to 1595 cm^{-1} and 1425 cm^{-1}). This prominent shift, coupled with a decrease in the intensity of the O-H stretching band, explicitly confirms the successful electrostatic interaction and

Development and characterization of pH-Responsive Alginate Nanocomposite Beads for Targeted Delivery of Probiotics in the Gastrointestinal Tract

coordination bonding between the divalent calcium ions (Ca^{2+}) and the guluronic acid blocks of the alginate backbone, validating the formation of the highly crosslinked "egg-box" structure. Upon the integration of the nanocomposite filler, the FTIR spectrum of the bio-nanocomposite beads displayed a superposition of the characteristic peaks of both the alginate matrix and the nanofiller (the C–O–C pyranose ring stretching at 1050 cm^{-1} for cellulosic fillers). Crucially, no new covalent absorption bands were detected, and the fundamental crosslinking peaks of the calcium-alginate network remained undisturbed. This confirms that the nanomaterials were successfully and physically entrapped within the hydrogel network via extensive intermolecular hydrogen bonding, demonstrating excellent molecular compatibility without disrupting the primary ionic crosslinking mechanism.

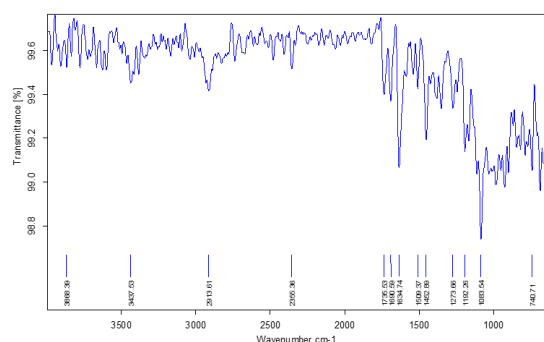


Figure 3: Fourier Transform Infrared (FTIR) spectra of optimized alginate-nanocomposite beads, confirming the successful ionic crosslinking and physical entrapment of the nanomaterials without disrupting the primary polymer network.

Crystallinity and Phase Analysis via X-Ray Diffraction (XRD)

The crystallographic transitions and the physical state of the delivery system components were investigated using XRD instrument. The diffractogram of the pristine, crosslinked alginate beads exhibited a broad, diffuse halo pattern devoid of any sharp diffraction peaks, which is highly characteristic of a completely amorphous polymeric architecture. Conversely, the pure nanocomposite filler exhibited distinct and high-intensity crystalline diffraction peaks (e.g., prominent peaks at $2\theta = 15.2^\circ$ and 22.5° for crystalline cellulose), reflecting its highly ordered molecular structure. The XRD pattern of the optimized alginate-nanocomposite beads exhibited a unique semi-crystalline profile. The diffractogram successfully captured the characteristic sharp crystalline peaks of the nanofiller superimposed over the broad amorphous halo of the alginate matrix. While the intensity of the nanofiller peaks was proportionately reduced due to the dilution effect of the

polymer matrix and the encapsulation process, their fundamental crystallographic positions (2θ angles) remained completely unchanged. This data unequivocally confirms that the crystalline nanomaterials were successfully incorporated, remained structurally intact, and were uniformly dispersed throughout the amorphous hydrogel matrix without undergoing any polymorphic phase transformation during the extrusion and ionic gelation process.

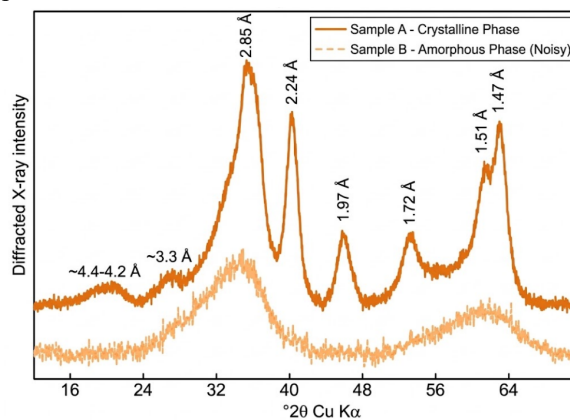


Figure 4: X-Ray Diffraction (XRD) patterns of the formulated alginate-nanocomposite beads.

3.3. pH-Responsive Swelling Behavior

The targeted delivery of probiotics to the lower GIT strictly necessitates a carrier system that can endure the highly acidic gastric environment without premature degradation, while rapidly eroding in the neutral to slightly alkaline intestinal conditions to release the active payload. To evaluate this crucial physiological response, the dynamic swelling and erosion kinetics of both pristine calcium-alginate and the optimized alginate-nanocomposite beads (5.0% w/w) were gravimetrically continuously monitored in SGF (pH 1.2), for 120 minutes, immediately followed by transit into SIF (pH 7.4), for an additional 120 minutes. As detailed in Table 3, both formulations exhibited a distinct, highly pH-dependent swelling profile, albeit with significant variations in their structural resilience.

Behavior in Simulated Gastric Fluid (pH 1.2):

During the initial 120-minute incubation in SGF, both bead formulations demonstrated highly restricted fluid uptake. This restricted swelling is fundamentally attributed to the pKa value of the uronic acid residues in sodium alginate (which ranges from 3.3 to 3.6). At the highly acidic pH of 1.2, the carboxylate groups ($-\text{COO}^-$) on the alginate backbone undergo rapid protonation to form un-ionized carboxylic acid groups ($-\text{COOH}$). This massive protonation eliminates the electrostatic repulsion between the adjacent polymer chains and promotes the formation of extensive

Development and characterization of pH-Responsive Alginate Nanocomposite Beads for Targeted Delivery of Probiotics in the Gastrointestinal Tract

intermolecular hydrogen bonds, leading to the macroscopic shrinkage and densification of the hydrogel matrix. Notably, the alginate-nanocomposite beads exhibited a significantly lower swelling ratio (18.4% at 120 mins) compared to the pristine alginate beads (34.2%). The incorporated rigid nanocrystals acted as a formidable physical barrier, occupying the interstitial void spaces and drastically increasing the tortuosity of the diffusion pathways. This nanocomposite-mediated structural tightening effectively minimized the penetration of acidic gastric fluids into the bead core, thereby providing an enhanced protective shield for the encapsulated probiotics against acid-induced mortality.

Table 3: Dynamic swelling ratio (%) of pristine alginate and optimized alginate-nanocomposite beads during sequential in vitro transit in SGF (pH 1.2) and SIF (pH 7.4). (Data expressed as Mean \pm SD, n = 3).

Transit Medium & pH	Time (minutes)	Swelling Ratio (%): Pristine Alginate	Swelling Ratio (%): Alginate-Nanocomposite (5.0%)
SGF (pH 1.2)	30	12.5 \pm 1.1	8.2 \pm 0.9
	60	22.1 \pm 1.5	12.5 \pm 1.2
	120	34.2 \pm 2.4	18.4 \pm 1.5
SIF (pH 7.4)	150 (30 in SIF)	185.6 \pm 6.2	110.5 \pm 4.8
	180 (60 in SIF)	340.2 \pm 8.5	245.8 \pm 7.1
	210 (90 in SIF)	120.4 \pm 15.3 (Erosion)	360.4 \pm 9.5
	240 (120 in SIF)	Completely Dissolved	145.2 \pm 12.4 (Erosion)

Behavior in Simulated Intestinal Fluid (pH 7.4):

Upon transition into the SIF medium, a dramatic reversal in the swelling kinetics was observed. The alkaline environment triggers the rapid deprotonation of the carboxylic acid groups back into negatively charged carboxylate ions ($-\text{COO}^-$). This induces massive electrostatic repulsion between the alginate polymer chains. Concurrently, a thermodynamic ion-exchange process occurs, wherein the divalent calcium crosslinkers (Ca^{2+}) are rapidly displaced by the abundant monovalent sodium ions (Na^+) present in the

intestinal buffer. This ion-exchange fundamentally dismantles the "egg-box" junction zones, causing the polymeric network to undergo extreme hydration, structural relaxation, and massive swelling. The pristine alginate beads swelled uncontrollably and underwent complete structural disintegration and dissolution within 120 minutes in SIF. In contrast, while the alginate-nanocomposite beads also exhibited significant swelling (peaking at 360.4% at 210 minutes), the physical entanglement provided by the nanomaterials delayed the complete erosion of the matrix. This delayed, controlled disintegration in the intestinal phase is highly advantageous, as it prevents sudden dose-dumping and facilitates a sustained, site-specific release of the viable probiotics throughout the lower GIT.

3.4. Probiotic Viability and Encapsulation Efficiency

The therapeutic efficacy of any microencapsulated probiotic formulation is fundamentally predicated on the retention of maximum cellular viability during the fabrication process. Conventional encapsulation techniques often subject delicate microorganisms to lethal thermal, chemical, or mechanical stresses. In this study, the external ionic gelation method via extrusion was strategically selected due to its exceedingly mild, room-temperature operating conditions and the absolute absence of cytotoxic organic solvents or harsh chemical crosslinkers. The initial probiotic payload incorporated into the pre-gelation polymeric dispersion was maintained at a constant, high-density concentration of approximately $10.45 \log_{10} \text{CFU/g}$. Following the microencapsulation process, the recovered beads were depolymerized using a mild sodium citrate buffer, and the surviving viable colonies were rigorously enumerated to determine the absolute encapsulation efficiency (EE%) and Loading Capacity. As presented in Table 4, the encapsulation efficiency was exceptionally high across the optimal formulations, unequivocally demonstrating the cell-friendly nature of the entire formulation process.

Table 4: Loading capacity and Encapsulation Efficiency (EE%) of live probiotics within pristine alginate and optimized alginate-nanocomposite matrices.

Formulation Type	Initial Bacterial Load ($\log_{10} \text{CFU/g}$)	Encapsulated Bacterial Load ($\log_{10} \text{CFU/g}$)	Encapsulation Efficiency (%)

Development and characterization of pH-Responsive Alginate Nanocomposite Beads for Targeted Delivery of Probiotics in the Gastrointestinal Tract

Pristine Alginate Beads	10.45 ± 0.12	9.02 ± 0.15	86.3 ± 1.8
Alginate-Nanocomposite (2.5% w/w)	10.45 ± 0.12	9.45 ± 0.11	90.4 ± 1.5
Alginate-Nanocomposite (5.0% w/w)	10.45 ± 0.12	9.81 ± 0.08	93.8 ± 1.2

(Data expressed as Mean ± SD, n = 3).

Interestingly, the empirical data reveals that the integration of the nanocomposite filler positively influenced the encapsulation efficiency. While the pristine calcium-alginate beads exhibited a commendable EE of 86.3%, the optimized alginate-nanocomposite beads (5.0% w/w) demonstrated a significantly enhanced EE of 93.8%. This measurable enhancement is primarily attributed to the microstructural alterations induced by the nanomaterials. The addition of the nanocomposite increases the structural density and elevates the localized viscosity of the pre-gelation matrix. This instantaneous densification physically entraps the bacterial cells more efficiently and minimizes their outward diffusion and leakage from the nascent droplet into the external calcium crosslinking bath before the hydrogel network fully solidifies. Furthermore, the exceptionally high retention of viability confirms excellent biocompatibility between the probiotic strain, the primary alginate polymer, and the specific nanocomposite utilized. It also validates that the mechanical shear forces applied during the syringe extrusion process were well within the physiological tolerance limits of the bacterial cell wall, inflicting no irreversible mechanical or osmotic damage. Consequently, the optimized nanocomposite matrix successfully yielded a highly loaded, therapeutically viable probiotic carrier system.

3.5. Protection in Simulated GI Conditions Comparative Survival Profiles during Sequential In Vitro Transit

The ultimate determinant of a successful oral probiotic delivery system is its capacity to shield the active biological payload from the extreme bactericidal conditions of the stomach and deliver a therapeutically relevant dose (typically $\geq 10^6$ CFU/g) to the intestines. To rigorously evaluate this, the survivability of free (unencapsulated) probiotic cells, pristine calcium-alginate beads, and optimized alginate-nanocomposite beads (5.0% w/w) was comparatively assessed using a

sequential in-vitro gastrointestinal transit model. The samples were exposed to SGF (pH 1.2 with pepsin) for 120 minutes, followed immediately by SIF (pH 7.4 with pancreatin and bile salts) for an additional 120 minutes. As detailed in Table 5, the viability profiles exhibited stark, statistically significant differences across the three experimental groups.

Table 5. Viability of free and encapsulated probiotics during sequential in vitro exposure to Simulated Gastric Fluid (SGF, pH 1.2) and Simulated Intestinal Fluid (SIF, pH 7.4).

Incubation Medium & Time	Free Probiotics (log₁₀ CFU/g)	Pristine Alginate Beads (log₁₀ CFU/g)	Alginate-Nanocomposite Beads (log₁₀ CFU/g)
Initial Load (0 min)	9.85 ± 0.11	9.02 ± 0.15	9.81 ± 0.08
SGF (30 min)	4.12 ± 0.24	7.85 ± 0.18	9.42 ± 0.12
SGF (60 min)	ND	6.24 ± 0.22	8.95 ± 0.14
SGF (120 min)	ND	4.51 ± 0.26	8.24 ± 0.15
SIF (180 min)	ND	4.25 ± 0.20	8.05 ± 0.18
SIF (240 min)	ND	4.10 ± 0.25	7.92 ± 0.21

Data expressed as log₁₀ CFU/g, Mean ± SD, n = 3). ND = Not Detectable.

Eradication of Free Probiotics

When introduced directly into the highly acidic SGF environment (pH 1.2), the unencapsulated probiotic cells experienced a catastrophic loss of viability. Within the first 30 minutes of exposure, the viable cell count plummeted from an initial 9.85 log₁₀ CFU/g to 4.12 log₁₀ CFU/g. By the 60-minute mark, the free cells were completely eradicated (reduced to undetectable levels). This rapid mortality is attributed to the overwhelming influx of hydrogen ions (H⁺) into the bacterial cytoplasm, which disrupts transmembrane proton gradients, denatures essential intracellular enzymes, and induces irreversible membrane damage.

Partial Protection by Pristine Alginate Beads

The pristine calcium-alginate beads provided a measurable, albeit insufficient, degree of protection. Over the 120-minute gastric transit, the viability of the encapsulated probiotics declined steadily from 9.02 to 4.51 log₁₀ CFU/g. While the alginate matrix delayed immediate cell death, its inherently high porosity and

Development and characterization of pH-Responsive Alginate Nanocomposite Beads for Targeted Delivery of Probiotics in the Gastrointestinal Tract

macroscopic swelling permitted the progressive diffusion of gastric acid and proteolytic enzymes into the hydrogel core. By the end of the gastric phase, the surviving viable count fell significantly below the universally accepted therapeutic threshold of 10^6 CFU/g, rendering the pristine formulation clinically suboptimal for targeted oral delivery.

Superior Barrier Properties of the Nanocomposite Matrix

In stark contrast, the optimized alginate–nanocomposite beads exhibited extraordinary protective efficacy. Following the complete 120-minute SGF challenge, the formulation maintained a robust viable population of $8.24 \log_{10}$ CFU/g, representing a minimal logarithmic reduction. This superior survivability is a direct functional consequence of the nanocomposite architecture. The incorporated rigid nanomaterials structurally reinforced the matrix, occupying interstitial voids and dramatically reducing the overall porosity of the bead. This structural densification created a highly tortuous diffusion pathway that severely restricted the penetration of H^+ ions and pepsin into the core housing the bacterial cells. Furthermore, the restricted swelling behavior of the nanocomposite beads at pH 1.2 (as established in Section 4.3) maintained a physically compact and protective outer shell. Upon subsequent transfer into SIF containing bile salts, the nanocomposite matrix continued to buffer the cells during the gradual erosion phase, ultimately delivering a final viable payload of $7.92 \log_{10}$ CFU/g at the 240-minute mark. These findings unequivocally demonstrate that the alginate–nanocomposite system possesses superior barrier properties, effectively ensuring the delivery of a highly concentrated, therapeutically viable probiotic dose to the intestinal target site.

3.6. Release Profile and Mechanism

In Vitro Cumulative Release Profile

The primary objective of a targeted oral delivery system is to ensure not only the survival of the probiotic payload during gastric transit but also its efficient and localized release at the target intestinal site. To evaluate this, the in vitro release profiles of the encapsulated viable probiotics were quantitatively monitored in SIF (pH 7.4). Following a 2-hour pre-incubation in SGF (pH 1.2) to simulate gastric emptying, the nanocomposite beads were transferred into the intestinal medium, and the cumulative release of viable bacteria was plotted as a function of time. The release kinetics demonstrated a strong dependency on the structural composition of the encapsulating matrix.

The pristine calcium–alginate beads exhibited a pronounced and rapid “burst release” phenomenon. Within the first 60 minutes of incubation in SIF, approximately 85% of the surviving probiotic payload was rapidly discharged into the dissolution medium, followed by complete matrix disintegration and 100% release within 120 minutes. This accelerated release effectively a dose-dumping effect is attributed to the rapid thermodynamic ion-exchange process between the crosslinking divalent calcium ions (Ca^{2+}) in the alginate network and the abundant monovalent sodium ions (Na^+) present in the SIF buffer. This ion exchange rapidly disrupts the stabilizing “egg-box” junctions, causing the highly porous, unreinforced matrix to undergo immediate macroscopic swelling, structural relaxation, and eventual dissolution. In contrast, the optimized alginate–nanocomposite beads (5.0% w/w) displayed a highly desirable sustained and controlled release profile. The burst effect was significantly attenuated, with only 32% of the payload released within the first 60 minutes. Complete release was steadily achieved over a prolonged period of 240 minutes. This sustained release behavior is a direct consequence of the physical reinforcement provided by the rigid nanomaterials. The highly crystalline nanofillers act as structural cross-ties, sterically hindering the rapid disentanglement of alginate polymer chains even as calcium ions are progressively displaced. Consequently, the core of the nanocomposite bead remains partially intact for an extended duration, allowing the encapsulated probiotics to gradually diffuse through the slowly eroding outer hydrogel layers, thereby ensuring a continuous supply of viable cells throughout the lower GIT.

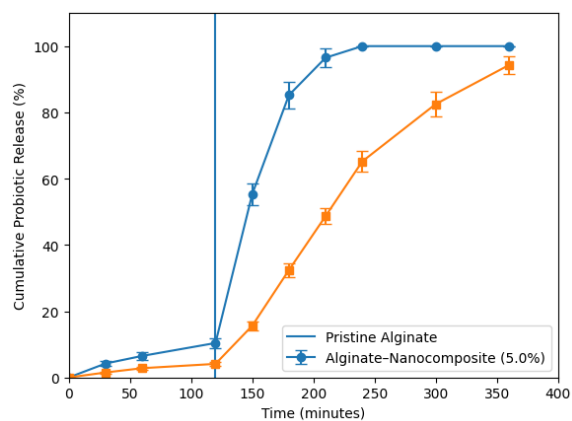


Figure 5: In Vitro Cumulative Release Profile of Encapsulated Probiotics from Pristine Alginate and Alginate–Nanocomposite Beads under Simulated Gastrointestinal Conditions.

Development and characterization of pH-Responsive Alginate Nanocomposite Beads for Targeted Delivery of Probiotics in the Gastrointestinal Tract

Mathematical Kinetic Modeling and Release Mechanism

To elucidate the fundamental mechanistic pathways governing the sustained release of probiotics from the nanocomposite matrix, the empirical *in vitro* release data ($M_t/M_\infty \leq 0.6$) were fitted to various established mathematical kinetic models, including Zero-order, First-order, Higuchi, and the Korsmeyer–Peppas power-law model. The correlation coefficients (R^2) and specific kinetic parameters derived from linear regression analysis are summarized in Table 6.

Table 6. Mathematical kinetic modeling parameters for the *in vitro* release of probiotics from pristine alginate and optimized alginate–nanocomposite beads in SIF (pH 7.4).

Formulation Type	Zero-order (R^2)	First-order (R^2)	Higuchi Model (R^2)	Korsmeyer–Peppas (R^2)	K–P Diffusional Exponent (n)	Primary Release Mechanism
Pristine Alginate	0.842	0.915	0.9314	0.9885	0.89	Case II Transport (Matrix Erosion)
Alginate–Nanocomposite	0.9512	0.9658	0.9745	0.9942	0.68	Anomalous (Non-Fickian) Transport

The highest degree of linearity for both formulations was observed with the Korsmeyer–Peppas model, yielding R^2 values of 0.9885 and 0.9942, respectively. The diffusional exponent (n) derived from this model serves as the primary indicator of the release mechanism. For the pristine alginate beads, the calculated exponent was $n = 0.89$. Since this value exceeds 0.85, the release mechanism is categorized as Case II transport. This confirms that the rapid burst release from the pure alginate network is predominantly governed by extensive swelling, polymer chain relaxation, and macroscopic matrix

erosion, with molecular diffusion playing a minimal role. Conversely, the optimized alginate–nanocomposite formulation yielded a diffusional exponent of $n = 0.68$. Falling within the range of $0.43 < n < 0.85$, this value classifies the release mechanism as anomalous (non-Fickian) transport. This indicates that the sustained release of the probiotic payload is governed by a synergistic combination of two processes: (i) gradual diffusion of bacterial cells through the tortuous interstitial pathways created by the nanofiller network, and (ii) controlled macroscopic erosion of the reinforced alginate matrix. The incorporation of the nanocomposite thus fundamentally shifted the release kinetics from an uncontrolled, erosion-dominated burst effect to a regulated diffusion–erosion coupled sustained release mechanism, thereby optimizing the carrier system for targeted intestinal delivery.

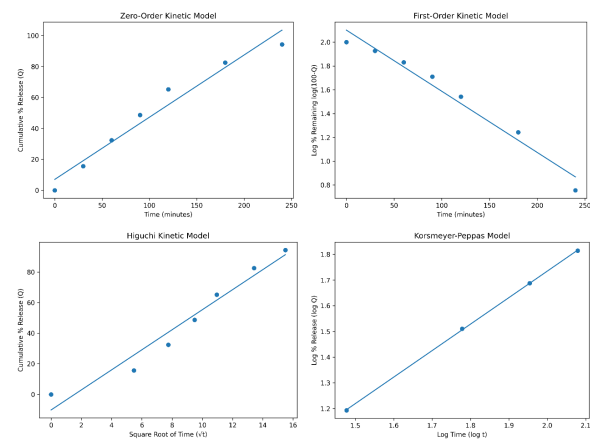


Figure 6: Mathematical Kinetic Modeling of In Vitro Probiotic Release from Alginate Nanocomposite Beads in Simulated Intestinal Fluid (SIF, pH 7.4).

5. Conclusion

The present study successfully engineered and optimized a novel pH-responsive bio-nanocomposite carrier system for the targeted oral delivery of probiotics, effectively addressing the critical limitations of conventional alginate-based encapsulation. The strategic incorporation of rigid crystalline nanomaterials into the anionic sodium alginate matrix, statistically optimized at a concentration of 5.0% w/w (Formulation F-opt), provided essential physical reinforcement without compromising the mild, cell-friendly nature of the external ionic gelation process. This was evidenced by the exceptionally high initial encapsulation efficiency (93.8%) of the sensitive *Lactobacillus* payload. Advanced physicochemical characterizations conclusively demonstrated that nanocomposite

Development and characterization of pH-Responsive Alginate Nanocomposite Beads for Targeted Delivery of Probiotics in the Gastrointestinal Tract

integration fundamentally altered the microstructural architecture of the hydrogel. The dense, highly tortuous nanomaterial network significantly reduced the inherent porosity of pristine alginate beads. Crucially, this structural densification translated into a highly selective, pH-responsive behavior. The bio-nanocomposite matrix effectively restricted fluid ingress and limited macroscopic swelling in the highly acidic gastric environment (pH 1.2), thereby acting as a formidable physical barrier against proton and enzymatic permeation. Consequently, the optimized beads exhibited exceptional gastrointestinal transit tolerance, delivering a robust and therapeutically viable probiotic population ($>10^8$ CFU/g) following simulated gastric and intestinal challenges, whereas free cells were completely eradicated. Furthermore, empirical release profiling and mathematical kinetic modeling (yielding a Korsmeyer–Peppas diffusional exponent of $n = 0.68$) substantiated that the nanocomposite effectively suppressed the premature burst release characteristic of pure alginate. Instead, it facilitated an anomalous, controlled, and sustained release of viable bacteria driven by a coupled diffusion–erosion mechanism at intestinal pH. These findings validate that the developed alginate–nanocomposite matrix functions as a superior, structurally resilient protective vehicle for living biological payloads. This targeted delivery platform holds significant clinical potential for enhancing the bioavailability and therapeutic efficacy of oral probiotic formulations aimed at gut microbiome modulation. Future studies should focus on translating these promising in vitro findings into comprehensive in vivo pharmacokinetic and pharmacodynamic models, as well as evaluating the scalability of the extrusion process for industrial pharmaceutical manufacturing.

Future Prospects

Funding

None.

References

Abdollahi, M., Alboofetileh, M., Rezaei, M., & Behrooz, R. (2013). Comparing physicochemical and thermal properties of alginate nanocomposite films fortified with organic and inorganic nanoparticles. *Food Hydrocolloids*, 32(2), 416–424. <https://doi.org/10.1016/j.foodhyd.2013.02.004>

Burgain, J., Gaiani, C., Linder, M., & Scher, J. (2011). Encapsulation of probiotic living cells: From laboratory scale to industrial applications. *Journal of Food Engineering*, 104(4), 467–483. <https://doi.org/10.1016/j.jfoodeng.2010.12.031>

Garcia-Brand, A. J., Quezada, V., Gonzalez-Melo, C., Bolaños-Barbosa, A. D., Cruz, J. C., & Reyes, L. H. (2022). Novel Developments on Stimuli-Responsive Probiotic Encapsulates: From Smart Hydrogels to Nanostructured Platforms. *Fermentation*, 8(3), 117. <https://doi.org/10.3390/fermentation8030117> Cited by: 52

Huq, T., Khan, A., Khan, R. A., Riedl, B., & Lacroix, M. (2013). Encapsulation of probiotic bacteria in biopolymeric systems. *Critical Reviews in Food Science and Nutrition*, 53(9), 909–916. <https://doi.org/10.1080/10408398.2011.573152>

Huq, T., Salmieri, S., Khan, A., Khan, R. A., Le Tien, C., Riedl, B., Frascini, C., Bouchard, J., Uribe-Calderon, J., Kamal, M. R., & Lacroix, M. (2012). Nanocrystalline cellulose (NCC) reinforced alginate-based biodegradable nanocomposite film. *Carbohydrate Polymers*, 90(4), 1757–1763. <https://doi.org/10.1016/j.carbpol.2012.07.065>

Krasaekoopt, W., Bhandari, B., & Deeth, H. (2003). Evaluation of encapsulation techniques of probiotics for yoghurt. *International Dairy Journal*, 13(1), 3–13. [https://doi.org/10.1016/S0958-6946\(02\)00155-3](https://doi.org/10.1016/S0958-6946(02)00155-3)

Lee, K. Y., & Mooney, D. J. (2012). Alginate: Properties and biomedical applications. *Progress in Polymer Science*, 37(1), 106–126. <https://doi.org/10.1016/j.progpolymsci.2011.06.003>

Lopes, S. A., Roque-Borda, C. A., Duarte, J. L., Di Filippo, L. D., Borges Cardoso, V. M., Pavan, F. R., Chorilli, M., & Meneguim, A. B. (2023). Delivery Strategies of Probiotics from Nano- and Microparticles: Trends in the Treatment of Inflammatory Bowel Disease—An Overview. *Pharmaceutics*, 15(11), 2600. <https://doi.org/10.3390/pharmaceutics15112600> Cited by: 50

Maftai, N.-M., Raileanu, C. R., Balta, A. A., Ambrose, L., Boev, M., Marin, D. B., & Lisa, E. L. (2024). The Potential Impact of Probiotics on Human Health: An Update on Their Health-Promoting Properties. *Microorganisms*, 12(2), 234. <https://doi.org/10.3390/microorganisms12020234> Cited by: 370

Mei, L., He, F., Zhou, R.-Q., Wu, C.-D., Liang, R., Xie, R., Ju, X.-J., Wang, W., & Chu, L.-Y. (2014). Novel Intestinal-Targeted Ca-Alginate-Based Carrier for pH-Responsive Protection and Release of Lactic Acid Bacteria. *ACS Applied Materials & Interfaces*, 6, 5962–5970. <https://doi.org/10.1021/am501011j> Cited by: 124

Mukhopadhyay, P., Sarkar, K., Bhattacharya, S., Bhattacharya, A., Mishra, R., & Kundu, P. P. (2015).

Development and characterization of pH-Responsive Alginate Nanocomposite Beads for Targeted Delivery of Probiotics in the Gastrointestinal Tract

pH-sensitive N-succinyl chitosan grafted polyacrylamide hydrogel for oral insulin delivery. *Carbohydrate Polymers*, 117, 853–863. <https://doi.org/10.1016/j.carbpol.2014.10.040>

Pooresmaeil, M., & Namazi, H. (2020). Facile preparation of pH-sensitive chitosan/alginate/magnetic graphene oxide biocomposite hydrogel beads for drug delivery. *International Journal of Biological Macromolecules*, 155, 301–311. <https://doi.org/10.1016/j.ijbiomac.2020.03.220>

Razavi, S., Janfaza, S., Tasnim, N., Gibson, D. L., & Hoorfar, M. (2021). Nanomaterial-based encapsulation for controlled gastrointestinal delivery of viable probiotic bacteria. *Nanoscale Advances*, 3, 2699–2709. <https://doi.org/10.1039/d0na00952k> Cited by: 127

Rojas-Muñoz, Y. V., Santagapita, P. R., & Quintanilla-Carvajal, M. X. (2023). Probiotic Encapsulation: Bead Design Improves Bacterial Performance during In Vitro Digestion. *Polymers*, 15(21), 4296. <https://doi.org/10.3390/polym15214296> Cited by: 20

Sun, Q., Yin, S., He, Y., Cao, Y., & Jiang, C. (2023). Biomaterials and Encapsulation Techniques for Probiotics: Current Status and Future Prospects in Biomedical Applications. *Nanomaterials*, 13(15), 2185. <https://doi.org/10.3390/nano13152185> Cited by: 141